Mechanisms behind pH changes during electrocoagulation

Weiss, Søren Fredberg; Christensen, Morten Lykkegaard; Jørgensen, Mads Koustrup

Published in:
AIChE Journal

DOI (link to publication from Publisher):
10.1002/aic.17384

Publication date:
2021

Document Version
Accepted author manuscript, peer reviewed version

AIChE J

DOI10.1002/aic.17384

Mechanisms behind pH changes during electrocoagulation

Søren Fredberg Weiss, Morten Lykkegaard Christensen, Mads Koustrup Jørgensen*

Center for Membrane Technology, Department of Chemistry and Bioscience, Aalborg University, Fredrik Bajers Vej 7H, DK-9220 Aalborg Øst, Denmark

*Correspondence: mkj@bio.aau.dk

Abstract

Electrocoagulation is a promising method for removing pollutants from surface water and industrial wastewater. The coagulation efficiency is dependent on pH but it is not fully understood how electrocoagulation affects pH of the treated water. Three series of experiments have been conducted to study how 1) chloride and sulphate anions, 2) negatively charged organic macromolecules and 3) carbonate influence pH during electrocoagulation. It is found that dissolved carbonate has a significant influence on the pH change as CO_2 is stripped off during electrocoagulation due to formation of H_2 microbubbles at the cathode. The pH increased by ~1 pH unit, which may significantly affect coagulation efficiency of iron. The pH increase depended strongly on the initial pH and the concentration of carbonate in the water. A secondary contribution to pH change was found to be ion exchange by sulfate and chloride ions into $Fe(OH)_3$ flocs, whereby OH^- was released into solution but only minor pH change was observed, not enough to affect the coagulation. The presence of charged organic macromolecules did not have any significant effect on pH.

Keywords: Electrochemical processes, surface water, flocculation, iron chemistry, water treatment, electrolysis

This article has been accepted for publication and undergone full peer review but has not been through the copyediting, typesetting, pagination and proofreading process which may lead to differences between this version and the Version of Record. Please cite this article as doi: 10.1002/aic.17384
Received: Jan 29, 2021;Revised: Apr 28, 2021;Accepted: Jul 07, 2021

1. Introduction

Water treatment is essential for the modern world, in terms of treating both industrial and domestic wastewater, and purification of water for use as potable water. As an example surface waters usually require treatment to remove pathogens, colloidal particles, humic acids, or nutrients before it is distributed to consumers [1,2]. A widespread method to treat the water is by coagulation followed by membrane filtration[3,4] or cake filtration [5].

Conventional chemical coagulation (CC) utilizes coagulants such as ferric or aluminum salts, which by various mechanisms are able to destabilize and remove colloidal particles [6]. The mechanism of the coagulation depends on numerous variables such as the specific nature of the coagulant, the dose of coagulant, and the pH of the influent water [6]. The drawbacks of conventional coagulation are primarily that addition of coagulant salts reduce pH [7,8]. As follows from the pH-pC diagram presented in Fig. 1, a change in pH affect coagulation efficiency, as the solubility of iron, concentration of iron species, charge of iron(III)hydroxide and the charge of flocs is pH dependent. It is therefore often necessary to regulate pH after addition of coagulant to maintain high coagulation efficiency at the application specific optimum pH level [6,9]. Further, addition of iron coagulant and adjustment of pH increases the concentration of chloride or sulfate anions, which for some applications is unwanted [10].

A different, and evolving technology for coagulation is electrocoagulation (EC). In EC, coagulant species are dissolved from a metal electrode without production of counterions, as metal ions form hydroxides and thereby remove the OH^- formed at the electrode. One of the metals most often used for EC is iron due to its high availability and high valence, where high valence is a critical parameter in coagulation efficiency [11]. A few key advantages and disadvantages of EC compared to CC are listed in Table 1.

EC has been studied for a wide range of applications, including removal of pollutants such as natural organic matter, microorganisms, several metals and nutrients from surface waters, groundwaters and

industrial wastewaters[1–3,5,8,14]. It works best for dissolved matter and dilute suspensions because coagulation can occur on the electrode surfaces if the water contains suspended materials at high concentration. This results in fouling of the electrode which introduces significant mass transport limitations for iron species being released and should be avoided.

Several studies have documented a neutralizing effect of EC, meaning that at low initial pH values (pH < 7.5), the pH will rise, and at high initial pH values (pH > 8.5) the pH will decrease [17–27]. For example, Chen et al.[17] observed a large pH increase when the influent pH was 3-6. At higher initial pH values (8-12), the increase becomes less significant. At higher pH values, the pH decreases. In one experiment, the pH decreased from ∼10 to ∼9 at a charge loading of 640 C/L. The pH change may in some applications be beneficial, for some applications unimportant and for some applications be problematic for the coagulation process, as pH is shifted from the optimum pH value. The pH changes due to EC is not well-understood.

This study investigates the mechanism(s) that cause the change in pH during electrocoagulation. Understanding these mechanisms will allow exploitation of this feature to avoid costs associated with pH adjustment in connection with the coagulation process. Understanding the pH change makes it possible to predict the pH change and even exploit it for pH adjustment. In this study, the emphasis will be put on iron EC. Itis the most often used metal and studies have shown a larger pH change with iron electrodes compared to aluminum electrodes [18,20].

The following mechanisms have been suggested in literature to explain the changes in pH during EC;

1. Ion exchange between hydroxide ions in iron(III)hydroxide complexes and chloride or sulfate ions in solution [23–26].
2. Stripping of dissolved carbonate as CO_2 by hydrogen bubbles released at the cathode [18,20–22,25,26,28].

Another possible mechanism may be the possible direct reaction between ferrous ions released from the electrodes and organic matter, thus freeing hydroxide ions released at the cathode and thereby increase the pH.

2. Materials and Methods

2.1 Mechanisms behind ion pH changes during EC

In Supplementary Material, the fundamental reactions during Fe release and reaction with water during EC are presented. Fig. 2 summarizes the different proposed mechanisms underlying pH changes during EC, which are also explained in this section of the article.

2.1.1. Ion exchange mechanism

The first explanation the exchange of anions such as sulfate or chloride into the iron(III)hydroxide complexes (Fig 2a), thus releasing one (or several) hydroxide ions into solution to increase the pH [23–26] as follows from the reaction schemes in Eq. 1.

$$Fe(OH)_3(s) + xCl^- \rightleftharpoons Fe(OH)_{3-x}Cl_x + xOH^-$$

$$Fe(OH)_3(s) + xSO_4^{2-} \rightleftharpoons Fe(OH)_{3-2x}(SO_4)_x + 2xOH^- \quad (1)$$

Since these proposed reactions occur after release from the electrodes and is not directly linked to any EC specific reaction, this mechanism will also happen during conventional, chemical coagulation (CC). In CC, hydrolysis of Fe^{3+} to $Fe(OH)_3$ releases $3H^+$ ions (Eq. S5.1-4, Supplementary Material), which reduces the pH. Thus, releasing the hydroxide ions again through ion exchange would only negate the decline that was initially observed, rather than elevate the pH.

Releasing the hydroxide ions from the iron(III)hydroxide complexes again would therefore only serve to neutralize the protons released during initial hydrolysis of Fe^{3+}. In contrast to this is EC, where OH^- and Fe^{3+} are produced in stoichiometric amounts. Release of the hydroxide ions from iron(III)hydroxide complexes in this scenario, would increase pH.

2.1.1. Reaction with negatively charged organic matter

Negatively charged organic materials may also influence the iron chemistry and pH (Fig. 2b). Fe^{2+} or Fe^{3+} ions released from the electrodes during EC may be able to react directly with negatively charged organic matter before precipitation as iron hydroxides. Fe^{2+} and Fe^{3+} is able to form complexes with organic matter, both in solution and in e.g. soil samples [29–31]. This complexation of iron reduce formation of iron(III) hydroxide whereby hydroxyl ions from the cathode are left in solution whereby pH increase. An illustration of this proposed theory is seen in Fig. 2B, and the proposed reaction scheme can be seen in Eq. 2.

$$2R\text{-}COO^- + Fe^{2+} \rightleftharpoons (R\text{-}COO)_2Fe \quad (2)$$

2.1.1. Carbonate stripping

Another theory, which is acknowledged in different studies, is that the hydrogen gas formed at the cathode strips the $CO_2(aq)$ from solution as $CO_2(g)$ [18,20–22,25,26,28] (see Eq. 3.1). Removal of carbonate from solution leads to a corresponding pH increase, as it results in a shift in the equilibrium with carbonic acid (Eq. 3.2-4) [33], The mechanism of CO_2 stripping, illustrated in Fig. 2C [18,21,22,25,26], requires the presence of carbonic acid in solution.

$$CO_2(aq) \rightleftharpoons CO_2(g) \quad (3.1)$$

$$H_2CO_3 \rightleftharpoons CO_2(aq) + H_2O \quad (3.2)$$

$$HCO_3^- + H^+ \rightleftharpoons H_2CO_3,\ pK_a = 6.3 \quad (3.3)$$

$$CO_3^{2-} + H^+ \rightleftharpoons HCO_3^-,\ pK_a = 10.3 \quad (3.4)$$

The disturbance of the hydrogen bubbles can strip carbonate, because the hydrogen bubbles that are formed on the cathode are very small. The typical diameter is 5-45 µm at pH 7 for hydrogen bubbles formed at iron electrodes according to G. Chen [18]. This gives them a large surface area to volume ratio, and therefore a large interface with the water. In addition to this, the partial pressure of CO_2 inside the hydrogen bubbles is initially zero, hence there is a driving force for carbonate stripping into the hydrogen bubbles.

2.2 Materials

A water solution was prepared for the experiments by using a synthetic substitute for surface water, based the composition of Lake Esthwaite in England [34], but including 10 mg/L of humic acid (HA) (Acros Organics) to simulate the organic content of surface water and serve as an indicator of the coagulation efficiency. A summary of the composition can be seen in Table 2. The water composition was achieved by addition of $CaCl_2 \cdot 2H_2O$ (VWR Chemicals, 100%), KCl (Applichem, >99.5%), $Mg(NO_3)_2 \cdot 6H_2O$ (Fluka Chemika >99%), Na_2CO_3 (VWR Chemicals, 100%), Na_2SO_4 (VWR Chemicals, 100%) to deionized water and pH was adjusted to different initial values for EC experiments using 1 M NaOH (Acros Organics, 98%) or 1 M HCl (Fischer Scientific U.K.). The buffer capacity was kept constant in all experiments at 450 µeq/L, corresponding to the alkalinity of Lake Esthwaite[34]. Samples without carbonate were prepared using disodium hydrogen phosphate (VWR Chemicals, >99%) instead of carbonate to ensure a buffer capacity of

450 µeq/L. The alkalinity of surface waters varies greatly between different bodies of water, and 450 µeq/L is probably in the low end based on a map of the alkalinity of surface waters in the United States by Omernik and Powers [35].

2.2.1. Electrocoagulation Setup

EC treatment was performed in a continuous EC cell with an electrode area of 240 cm^2 (two sheets of 300x40 mm size and 1 mm thickness. Refer to Supplementary Material Fig. S2 for further details about the cell) in a monopolar configuration with a void volume of 130.0 mL.

2.3 Methods

2.3.1 Electrocoagulation Procedure

A feed tank containing 5 L of synthetic surface water was used for each experiments. The feed solution was pumped through the EC cell at a rate of 52 mL/min using a peristaltic pump (Watson Marlow Sci Q400). The current ranged from 30-150 mA, and the voltage between 0.9 V and 4.3 V with a DC power supply (Elektro-Automatik PS 2032-050). The retention time in the cell was kept constant during all experiments and was 2.5 minutes. A current was applied, and the first 260 mL of effluent was discarded (two void volumes). After this, a steady state condition was assumed, and effluent from the electrocoagulation cell, containing released Fe ions, was directed through a static inline mixer and then into a slow mixing tank to allow for flocculation (Fig. 3). The retention time in the stirring tank was minimum 25 minutes. After slow mixing in the stirring tank, the flocs were allowed to settle, and the absorbance of the supernatant at 650 nm was measured on a spectrophotometer (Thermo Scientific Helios ε). This was done to quantify the removal efficiency in terms of humic substances for the coagulation, and therefore ensure that the experiments were conducted under realistic circumstances.

2.3.2. Procedure for Determining the Magnitude of pH Changes During EC Operation

A series of experiments were conducted, to first investigate the magnitude of the pH changes that would occur during normal EC operation (procedure explained in detail in section 3.2.1). These experiments were conducted at influent pH values of 4.00, 5.00, 5.50, 6.00, 6.50, 7.00, and 8.00, and charge loadings of 35, 70, 105, 140, and 175 C/L (corresponding to Fe^{3+} doses of 10, 20, 30, 40, and 50 mg/L, assuming a 100 % current efficiency) and all combinations of these initial pH values and charge loadings. These experiments were run in triplicate. pH adjustments were carried out using 0.1M HCl. Any addition of chloride for acidification was compensated by adding less chloride salts, to keep the chloride concentration constant at 20 mg/L during all experiments.

A theoretical approach was used to study the potential impact of dissolution of iron in water. The chemistry of iron in water is complex, but at near-neutral pH values (pH 6-8), the solubility of iron is low and dissolved iron species exist only in trace amounts that by themselves are unlikely to significantly affect the pH of the system by remaining unhydrolyzed. It was assumed that equilibrium was established for the iron species. An estimation of the potential influence of iron dissolved from EC electrodes was based on the amount of OH^- released by the cathodes that is not neutralized by iron hydroxide formation. For example, 10^{-8} M Fe^{3+} in solution is equal to 310^{-8} M of OH^- release, while 10^{-8} M $FeOH^{2+}$ is equal to 210^{-8} M of OH^- release. The underlying data for the figures has been calculated both by using a chemical equilibrium program (Visual MINTEQ version 3.1; KTH, Stockholm, Sweden) and by using the data from pH-pC diagrams. Visual MINTEQ has a wide thermodynamic database and model default values were used for all equilibrium constants. The Davies method was used for activity corrections during simulations.

The potential mechanisms behind pH changes were investigated in experiments summarized in Table 3 and described in detail in sections 2.3.3 – 2.3.5.

2.3.3. Procedure for Investigating the Ion Exchange Mechanism

Different concentrations of either sulfate or chloride (concentrations: 10^{-4} M, 10^{-3} M, 10^{-2} M, and 10^{-1} M) were passed through the EC cell operated at 60 mA which corresponds to a charge loading of 70 C/L. The inlet pH of the feed was 6.00. The effluent was collected and placed in 500 mL containers on an orbital shaker at 250 rpm. The experiments were run in triplicates. A 3 mL sample was taken from the stirring tank at the start of the experiment, after 30 minutes, 1 hour, and 72 hours and filtered through a syringe filter (cellulose ester, pore size = 0.45 µm) to remove flocs. The pH was then immediately recorded, and the difference in pH from the initial value was calculated.

Furthermore, chemical equilibrium modelling was carried out in Visual MINTEQ (Ver. 3.1) to evaluate which iron species would form in water with the specific composition presented in Table 2, at pH values between 6 and 8. The aim of this was to investigate how many hydroxide ions in average were associated with ferric ions and hence determine pH increase resulting from hydroxide ions not associated with ferric ions.

2.3.4. Investigation of the Hydrogen Gas Stripping Mechanism

Two experiments were conducted to study carbonate stripping. A regular EC experiments was conducted with varying concentrations of carbonate in the water to measure the pH change at different initial carbonate concentrations. Three carbonate concentrations were tested at 0 µeq/L, 225 µeq/L and 450 µeq/L. Disodiumphosphate was added to a final concentration of carbonate plus phosphate of 450 µeq/L in order to keep the buffer capacity constant. See Table 4.

In the second experiment, the synthetic surface water was sparged with hydrogen in an isolated experiment. Hydrogen was generated at a relatively steady rate of 12 cm^3/min by addition of 0.1 M HCl to magnesium turnings. This rate of generation corresponds to the generation of H_2 in the EC cell with a

charge loading of 105 C/L. The gas was bubbled through a beaker containing synthetic surface water over a period of 20 minutes, continuously measuring the pH with a pH electrode (SI Analytics BlueLine). These experiments were conducted at an initial pH of 6.00, 7.00, and 8.00. For an illustration of the hydrogen generator setup, see Fig. 4.

Carbonate stripping as function of time was modelled mathematically. The partial pressure in the air bubbles was calculated from the equilibrium between carbonate in air and water, and by including the acid –base reaction of carbonate i.e. Eq. 3.2, 3.3. and 3.4). Henry's constant was set for carbon dioxide was set to 0.034 mol/(kg⋅bar), with the concentration of carbonate in solution in molal and partial pressure of carbon dioxide in the air bubbles in Pa. It was assumed that the total amount of carbonate in the water was constant and not affected by the mass transport to the air. A detailed description can be seen in Supplementary Material.

2.3.5. Investigation into the Potential Reactions Between Fe^{2+} and Organic Matter

Ferrous ions and varying concentration of dissolved organic macromolecules (HA) was tested to study how the reaction between iron and HA affect pH. Synthetic surface water was produced as described in Table 4 but without HA. The synthetic water without HA was treated in the EC cell operated at 120 mA which is twice the regular current level) and a charge loading of 140 C/L. After treatment, the treated water was mixed with synthetic surface water containing HA (50/50) to a final charge loading of 70 C/L. Samples was prepared with finale concentrations of HA of 0, 10, 20, and 40 mg/L. The procedure ensured that there was interaction between Fe^{2+} and organic matter, before the Fe^{2+} has been allowed to oxidize to Fe^{3+} and form iron(III)hydroxide flocs.

The pH of the mixture was measured after 25 minutes of slow stirring. The results in terms of pH change was then compared with references, conducted as described in section 2.1.1.

2.3.6 Calculation of H^+ consumption

The consumption of H^+ was calculated feed pH, pH after EC treatment, and the concentration of carbonate (Eq. 4-5). Carbonate is the only buffering system present in feed. The consumption of H^+ was calculated as the difference in H^+ concentration before and after EC treatment and the H^+ consumption due to the carbonate buffer:

$$\Delta[H^+] = (10^{-pH_i} - 10^{-pH_f}) + (([CO_2(aq)]_{pH=i} - [CO_2(aq)]_{pH=f}) + ([CO_3^{2-}]_{pH=f} - [CO_3^{2-}]_{pH=i})) \quad (5)$$

Where β is the buffer capacity, which is assumed only came from carbonate in water. The buffer capacity in Eq. 4 expresses the concentration change of H^+ due to reaction between H^+ and the carbonate buffer.

3. Results

3.1. Establishment of pH Change During EC

The pH change was determined during EC of synthetic surface water of varying pH values, all with a buffer capacity of 450 µeq/L. In Fig. 5a, the measured effluent pH is plotted against the influent pH for electrocoagulation with five different charge loadings. The mean effluent pH was higher than the influent pH except for samples with an influent pH of 8.00, where two of the data points are below the bisecting line.

The decline in concentration of H^+ has been calculated as function of influent pH (Fig. 5b) and was at a steady level between 10^{-4} and 2⍰10^{-4} M up to an influent pH of 6.5, above which the H^+ consumption declined significantly.

The decline in H^+ concentration after EC treatment is plotted against the charge loading (Fig. 6). The general trend is that the the decline in H^+ concentration increases until 70 C/L, above which the H^+ decline was

relatively constant with increasing charge loading. This indicates that the pH altering effect may already be saturated at low dose of iron.

Theoretical estimations of the impact of dissolved ferric ions on pH are shown in Fig. 7, both in terms of direct H^+ consumption due to the release of OH^- from cathodes and the difference in pH associated with that consumption. While there are differences between what is calculated from the pH-pC diagram and the MINTEQ calculations, the key point is that the pH change was negligible and cannot explain the pH change observed during EC.

The results in terms of humic acid removal efficiency and current efficiency were also measured for these experiments. They varied between 75-100 % and 82-98%, respectively, depending on the charge loading (and therefore iron dose) and the initial pH. These results can be found in Supplementary Material.

3.2. Ion Exchange Mechanism

The ion exchange mechanism was investigated by measuring the decline in H^+ concentration as function of chloride and sulfate concentrations in the feed (Fig. 8). The H^+ concentration decline is referred to as a consumption of H^+, as the elevation in pH is a result of H+ reacting, potentially through one of the proposed mechanisms. The inlet pH before the EC cell was 6.00, and the effluent pH varied between 5.77 and 6.25. The solid lines in Fig. 8 represent the maximum theoretical H^+ consumption. This was calculated from the assumption that all hydroxide is exchanged with every available Cl^-/SO_4^{2-} anion to form $FeCl_3/Fe_2(SO_4)_3$, and using the release of hydroxide ions from iron to calculate corresponding H^+ consumption. This effect is limited by the anion concentration at low concentrations and limited by the available of Fe^{3+} at high concentration. the maximum exchange of ions was calculated for two different common mineral structures for both chloride or sulphate. Chemical equilibrium modelling in Visual MINTEQ (Ver. 3.1) on water with the composition presented in Table 2 (pH values varying between 6 and 8) shows that species containing either sulfate or chloride (e.g. $KFe^{3+}{}_3(OH)_6(SO_4)_2$ or $Fe(OH)_{2.7}Cl_{0.3}$) are oversaturated in solution if no precipitation

occurs. This means that there must an equilibrium between precipitated $Fe(OH)_3(s)$ and dissolved $Fe^{3+}(aq)$ and these species, resulting in a de facto ion exchange. The maximum pH change effect in Fig. 8 for $KFe^{3+}{}_3(OH)_6(SO_4)_2$ or $Fe(OH)_{2.7}Cl_{0.3}$) shows the maximum consumption of H+ by ion exchange from $Fe(OH)_3$ into the respective species.

pH measurements show that the equilibria establish themselves quickly, with no significant change of H^+ concentration with time, all lower than for the potential full ion exchange of hydroxide ions with sulphate and chloride ions (Fig. 8). For both chloride and sulphate, it is not possible to discern any significant change in H^+ consumption as a function of anion concentration.

While it is peculiar that the concentrations of sulfate and chloride do not seem to influence the degree of ion exchange, this can perhaps be explained by the fact that, at pH = 6.00, the hydroxide concentration is 10^{-8} M, 10^4 times lower than the lowest concentration of sulfate or chloride tested. This 10^4 times disparity in concentrations could mean that at these anion concentration levels the equilibrium is independent of the anion concentration, because it is comparatively high already i.e. the equilibrium does not shift significantly when further chloride is added. This could also be the explanation for why the equilibrium is established so quickly, and no difference can be perceived for the different experimental durations.

3.3. Impact of Carbonate Concentration

The potential impact of carbonate being stripped from solution during EC was evaluated by varying the concentration of carbonate in solution while maintaining a constant buffer capacity in the system by compensating with phosphate. The change in pH before and after electrocoagulation is plotted against charge loading for the three different buffered systems in Fig. 9. The initial pH value of solutions was 6.00.

The results show that the pH of the solution with a 450 µeq/L carbonate buffer increases the most, followed by the buffer consisting of 225 µeq/L phosphate and 225 µeq/L carbonate, and finally the

phosphate buffered solution had the lowest elevation of pH by EC. This is consistent with the theory that the carbonate is evaporated as CO_2, since the largest pH changes occur when the carbonate concentration is the highest.

If all carbonate was stripped, and there was no buffering effect from the iron, a pH as high as ~10.5 could potentially be reached at a carbonate buffer capacity of 450 µeq/L. This means that nowhere near all the carbonate is removed. A ΔpH value of 0.5, corresponds to the removal of only roughly 50 µeq/L of carbonate.

In addition to the EC experiments presented in Fig. 9, the gas stripping mechanism was isolated by bubbling hydrogen from an external source through the synthetic surface water in an isolated jar test with no other variables, made with the three different buffer systems (carbonate buffer, 50/50 buffer, and phosphate buffer). The resulting development in pH over time at different initial pH values (pH = 6.00, 7.00 and 8.00) are presented in Fig. 10. The results from Fig. 9 have been added as an overlay to the pH 6 graph to compare the two.

The results show that when the initial pH is 6.00 or 7.00, the pH increases during bubbling with hydrogen gas. This increase is clearly dependent on the concentration of carbonate in the solution. It is seen that if the carbonate concentration is 0 µeq/L then the pH changes only slightly, with a ΔpH of roughly 0.1. As expected, the solution with 450 µeq/L carbonate exhibits the highest ΔpH of 0.8 at initial pH = 6.00, and 0.45 at initial pH = 7.00. The solution with 225 µeq/L carbonate lies between the two extremes. With an initial pH = 8.00, however, the pH decreases from bubbling with hydrogen gas. However, as seen in Fig. 10, when the pH reaches a value between 7 and 8 an opposing force lowering the pH is introduced, which along with the altered speciation of the carbonate system as a function of pH skews it away from the production of removable carbonic acid, explains why the potential pH increase is not fully achieved.

To confirm that carbonate is disappearing from solution, the alkalinity of the solutions were measured by standard titration to pH 4.5, after the bubbling treatments. The results from this can be seen in Fig. 11, which clearly shows a reduction in alkalinity over time, which in this controlled system can also be interpreted as a reduction in carbonate concentration.

The kinetics of the CO_2 transport during bubbling with hydrogen gas is dependent on the concentration of dissolved CO_2, which impacts the equilibrium partial pressure of gaseous CO_2. The solution pH determines the distribution of carbonate species, meaning that the higher the pH, the less of the carbonate exists as the volatile species CO_2(aq). Fig. 12 shows the theoretical equilibrium partial pressure of CO_2 as function of pH for solutions of different carbonate concentrations calculated by Henry's law. The graph shows higher equilibrium partial pressures of CO_2 with higher carbonate concentrations. When the pH approaches 7 and above, less than 5% of the carbonate in solution is present as dissolved CO_2, which reduces the equilibrium partial pressure as shown in Fig. 12. This will result in reduced carbonate stripping, hence less pH change at higher initial pH values.

3.4. Significance of Reaction Between Fe^{2+} and Organic Matter

The potential reactions between Fe^{2+} released by the electrodes directly with organic matter in solution is studied by comparing pH change values for regular in-situ (inline) EC experiments with EC experiments where the iron was dosed from a side stream containing no organic matter. The resulting pH changes for different humic acid concentrations and varying doses can be seen in Fig. 13.

It is not possible to distinguish the results from the inline configuration from the results from side stream configuration based on the pH change and there is no distinguishable trend in ΔpH as a function of the humic acid concentration (Fig. 13). For each of treatments (pH 6 and 7 and side-stream and in-line) a one-way ANOVA was carried out, showing no significant impact of HA concentration on the development in pH ($p > 0.05$ in all cases), confirming that HA concentration does not contribute to the magnitude pH change. These factors together lead to the conclusion that the presence of humic acids in this concentration range

does not significantly affect the pH of the treated water. It is possible to see a difference between the two initial pH values. When the initial pH value = 6.00, all of the experiments showed an increase in pH after EC treatment. This is not the case when initial pH = 7.00. At influent pH = 7.00, the ΔpH values are generally lower, but negative ΔpH values also occur. This is to be expected, since the pH = 7.00 samples are already neutral and, as seen in Fig. S4 (Supplementary Material), the pH increase during bubbling is only moderate when influent pH = 7.00.

4. Discussion

The largest pH change was observed during carbonate stripping, with a smaller contribution from hydroxide ions released from ion exchange with anions as chloride and sulphate. Organic macromolecules and their interaction of iron species in solution seemingly has no effect on pH. According to Abate and Masini [32] humic acids have a charge density of roughly 1-4 mmol/g depending on the pH of the solution, meaning that at a humic acid concentration of 10 mg/L and a pH of 7, 2.910^{-5} mol/L Fe charges may theoretically be neutralized by humic substances. However, in the present study this was not found to have a significant effect on the pH of the solutions.

The findings of this study complement and extend previous work by several authors who study the pH change that occurs during EC, and confirm a pH increase during EC when the influent pH is below 7. It is found that pH increases during EC, with higher elevation in pH at lower initial pH values and insignificant pH increase at initial pH values of 8. This is consistent with the results obtained by Adhoum et al. [23], Chen et al. [26], and Mouedhen et al. [25], that shows a decreasing pH if the influent pH is alkaline in industrial and restaurant wastewater. Hence EC seems to have a neutralizing effect to adjust pH to around 7-8. The higher pH changes reported in some literature studies may be due to higher charge loading than the present work (up to ~1100 C/L) [17,25]. However, other studies on wastewaters report that electrocoagulation operated in batch mode reaches higher pH levels (10-12) [5,36,37], with Fe electrodes resulting in higher pH values than Al

electrodes. One explanation for the decline in pH could be the dissolution of free Fe^{3+} ions not reacting to form ferric hydroxides, which would result in excess hydroxide ions being formed at the cathode to elevate pH. However, by simulating the amount of free Fe^{3+} ions, it was shown that this would lead to an insignificant elevation of pH (Fig. 7). Therefore, the equilibrium of Fe ions in water during EC establish quickly with an insignificant contribution to pH change.

The H^+ consumption is independent of the influent pH up to pH 5.5 after which it decreases (Fig. 5). This would disfavor theories such as the one proposed by Chen et al. [26], who suggest that the pH change is caused by ion exchange of chloride and sulfate ions into the iron hydroxide flocs, releasing hydroxide ions. This reaction is an equilibrium reaction that is expected to be dependent on the H^+ concentration; thus the extent of this reaction is expected to depend strongly on the pH. This conclusion is supported by data showing that the potential anion adsorption only has a minor effect on pH in this study probably because of the high carbonate concentration contributing to a buffer effect.

Stripping of carbonate as CO_2 is also dependent on the pH (Fig 12). When carbonate is stripped by the H_2 bubbles it is quickly removed due to the buoyancy, thus shifting the equilibrium towards production of more $CO_2(aq)$. Considering the pK_a of 6.3 for the equilibrium between $CO_2(aq)$ and HCO_3^-, at pH values higher than 7.5, there will be low concentration of removable $CO_2(aq)$ species present in solution and therefore a low equilibrium partial pressure of CO_2 (cf. Fig 12) resulting in the same positive feedback loop of removal and equilibrium reestablishment, but at a significantly slower rate as the pH increases. This agrees well with the observation from Fig. 5b, showing that H^+ consumption is constant below pH values of 5.5 and decreases at higher values. Hence, there is a correlation between the influence of initial pH values on the development in pH and carbonate solubility, that supports the mechanism of pH change by CO_2 stripping by the hydrogen bubbles formed at the cathode. However, it is shown that charge loading influences pH change up to a critical charge load (Fig. 6). This may be explained by fact that the hydrogen bubbles are only formed close to the cathode, thus limiting how much carbonate can be stripped from the water at low pH values.

If carbonate stripping was the only mechanism contributing to the pH change during EC, there should be no pH change for the phosphate buffered solutions with no carbonate. However, a modest pH change was observed, and that could potentially be caused by the contribution from the ion exchange between anions in water and hydroxide ions in $Fe(OH)_3$ flocs.

5. Conclusions

The objective of this paper was to elucidate the mechanisms that cause the pH changes that occur following treatment of waters with electrocoagulation.

Experiments have been conducted to determine the mechanisms behind the pH change and show that stripping of carbonate as CO_2 was the main contributor to the pH change during electrocoagulation. CO_2 stripping was due to the formation hydrogen gas at the cathode, which swept away CO_2 from solution as CO_2 gas. Experiments where the carbonate buffer is replaced with a phosphate buffer showed a negligible pH change.

Ion exchange between Cl^- or SO_4^{2-} and the hydroxide ions in iron(III)hydroxide flocs is a secondary, less significant contributor to pH change as a consequence of EC treatment. Experiments with different concentrations of chloride and sulfate in treated waters yielded results that in nearly all cases showed an increase in pH after ion exchange had occurred.

Furthermore, it was also discovered that hydrogen gas bubbles are at least partly responsible for the decrease in pH that occurs at initial pH > 8.

Acknowledgements

Timo Kirwa (Aalborg University) is acknowledged for building the EC cell.

Competing interest statement

The authors declare that there is no conflict of interest

6. References

1. El-Masry MH, Sadek OM, Mekhemer WK. Purification of raw surface water using electro-coagulation method. *Water Air Soil Pollut*. 2004;158(1):373-385. doi:10.1023/B:WATE.0000044857.02199.45

2. Payment P, Trudel M, Plante R. Elimination of viruses and indicator bacteria at each step of treatment during preparation of drinking water at seven water treatment plants. *Appl Environ Microbiol*. 1985;49(6):1418-1428. doi:10.1128/aem.49.6.1418-1428.1985

3. Bagga A, Chellam S, Clifford DA. Evaluation of iron chemical coagulation and electrocoagulation pretreatment for surface water microfiltration. *J Memb Sci*. 2008;309(1-2):82-93. doi:10.1016/j.memsci.2007.10.009

4. Crittenden JC. Coagulation and flocculation. In: *MWH's Water Treatment: Principles and Design*. Wiley; 2012:541-640.

5. Gafiullina A, Mamelkina M, Vehmaanperä P, Kinnarinen T, Häkkinen A. Pressure filtration properties of sludge generated in the electrochemical treatment of mining waters. *Water Res*. 2020;181. doi:10.1016/j.watres.2020.115922

6. Duan J, Gregory J. Coagulation by hydrolysing metal salts. *Adv Colloid Interface Sci*. 2003;100-102(SUPPL.):475-502. doi:10.1016/S0001-8686(02)00067-2

7. Eikebrokk B. Eikebrokk 1999, Coagulation-direct filtration of soft, low alkalinity humic waters.pdf. *Water Sci Technol*. 1999;40(9):55-62.

8. Cañizares P, Jiménez C, Martínez F, Rodrigo MA, Sáez C. The pH as a key parameter in the choice between coagulation and electrocoagulation for the treatment of wastewaters. *J Hazard Mater*.

2009;163(1):158-164. doi:10.1016/j.jhazmat.2008.06.073

9. Dovletoglou O, Philippopoulos C, Grigoropoulou H. Coagulation for treatment of paint industry wastewater. *J Environ Sci Heal - Part A*. 2002;37(7):1361-1377. doi:10.1081/ESE-120005992

10. Mollah MYA, Morkovsky P, Gomes JAG, Kesmez M, Parga J, Cocke DL. Fundamentals, present and future perspectives of electrocoagulation. *J Hazard Mater*. 2004;114(1-3):199-210. doi:10.1016/j.jhazmat.2004.08.009

11. Gregory J. *Coagulation and Flocculation*. London; 2005. doi:10.1680/bwtse.63341.061

12. Bazrafshan E, Mohammadi L, Ansari-Moghaddam A, Mahvi AH. Heavy metals removal from aqueous environments by electrocoagulation process - A systematic review. *J Environ Heal Sci Eng*. 2015;13(1). doi:10.1186/s40201-015-0233-8

13. Moussa DT, El-Naas MH, Nasser M, Al-Marri MJ. A comprehensive review of electrocoagulation for water treatment: Potentials and challenges. *J Environ Manage*. 2017;186:24-41. doi:10.1016/j.jenvman.2016.10.032

14. Bayramoglu M, Eyvaz M, Kobya M. Treatment of the textile wastewater by electrocoagulation. Economical evaluation. *Chem Eng J*. 2007;128(2-3):155-161. doi:10.1016/j.cej.2006.10.008

15. Espinoza-Quiñones FR, Fornari MMT, Módenes AN, et al. Pollutant removal from tannery effluent by electrocoagulation. *Chem Eng J*. 2009;151(1-3):59-65. doi:10.1016/j.cej.2009.01.043

16. Rodriguez, J.; Stopic, S.; Krause, G.; Friedrich B. Feasibility Assessment of Electrocoagulation Towards a New Sustainable Wastewater Treatment. *Environ Sci Pollut Res*. 2007;14(7):477-482.

17. Chen, Xueming; Chen Guohua; Yue PL. Separation of pollutants from restaurant wastewater by electrocoagulation. *Sep Purif Technol*. 2000;19:65-76. doi:10.1080/01496390601120557

18. Chen G. Electrochemical technologies in wastewater treatment. *Sep Purif Technol*. 2004;38(1):11-41.

doi:10.1016/j.seppur.2003.10.006

19. Hashim KS, Al Khaddar R, Jasim N, et al. Electrocoagulation as a green technology for phosphate removal from river water. *Sep Purif Technol*. 2019;210(April 2018):135-144. doi:10.1016/j.seppur.2018.07.056

20. Vepsäläinen M, Sillanpää M. Electrocoagulation in the treatment of industrial waters and wastewaters. *Adv Water Treat*. 2012. doi:10.1016/b978-0-12-819227-6.00001-2

21. Vik EA, Carlson DA, Eikum AS, Gjessing ET. Electrocoagulation of potable water. *Water Res*. 1984;18(11):1355-1360. doi:10.1016/0043-1354(84)90003-4

22. Kobya M, Senturk E, Bayramoglu M. Treatment of poultry slaughterhouse wastewaters by electrocoagulation. *J Hazard Mater*. 2006;133(1-3):172-176. doi:10.1016/j.jhazmat.2005.10.007

23. Adhoum N, Monser L, Bellakhal N, Belgaied JE. Treatment of electroplating wastewater containing Cu2+, Zn 2+ and Cr(VI) by electrocoagulation. *J Hazard Mater*. 2004;112(3):207-213. doi:10.1016/j.jhazmat.2004.04.018

24. Trompette JL, Vergnes H. On the crucial influence of some supporting electrolytes during electrocoagulation in the presence of aluminum electrodes. *J Hazard Mater*. 2009;163(2-3):1282-1288. doi:10.1016/j.jhazmat.2008.07.148

25. Mouedhen G, Feki M, Wery MDP, Ayedi HF. Behavior of aluminum electrodes in electrocoagulation process. *J Hazard Mater*. 2008;150(1):124-135. doi:10.1016/j.jhazmat.2007.04.090

26. Chen G, Chen X, Yue PL. Electrocoagulation and Electroflotation of Restaurant Wastewater. *J Environ Eng*. 2000;126(September):858-863.

27. Akyol A. Treatment of paint manufacturing wastewater by electrocoagulation. *Desalination*. 2012;285:91-99. doi:10.1016/j.desal.2011.09.039

28. Kobya M, Hiz H, Senturk E, Aydiner C, Demirbas E. Treatment of potato chips manufacturing wastewater by electrocoagulation. *Desalination*. 2006;190(1-3):201-211. doi:10.1016/j.desal.2005.10.006

29. Yamamoto M, Nishida A, Otsuka K, Komai T, Fukushima M. Evaluation of the binding of iron(II) to humic substances derived from a compost sample by a colorimetric method using ferrozine. *Bioresour Technol*. 2010;101(12):4456-4460. doi:10.1016/j.biortech.2010.01.050

30. Daugherty EE, Gilbert B, Nico PS, Borch T. Complexation and Redox Buffering of Iron(II) by Dissolved Organic Matter. *Environ Sci Technol*. 2017;51(19):11096-11104. doi:10.1021/acs.est.7b03152

31. Senesi N, Griffith SM, Schnitzer M, Townsend MG. Binding of Fe3+ by humic materials. *Geochim Cosmochim Acta*. 1977;41(7):969-976. doi:10.1016/0016-7037(77)90156-9

32. Abate G, Masini JC. Influence of pH and ionic strength on removal processes of a sedimentary humic acid in a suspension of vermiculite. *Colloids Surfaces A Physicochem Eng Asp*. 2003;226(1-3):25-34. doi:10.1016/S0927-7757(03)00418-7

33. Bohn, H. L., B. L. McNeal and GAO. Gas Dissolution. In: *Soil Chemistry*. 4th ed. Wiley; 2001:87.

34. S. C. Maberly, M. M. De Ville, H. Feuchtmayr, I. D. Jones, E. B. Mackay, L. May, S. J. Thackeray, I. J. Winfield. *The Limnology of Esthwaite Water : Historical Change and Its Causes , Current State and Prospects for the Future Lake Ecosystem Group , Lancaster Environment Centre , Library Avenue ,*. Lancaster; 2011.

35. Omernik JM, Powers CF. Total Alkalinity of Surface Waters-A National Map. *Ann Assoc Am Geogr*. 1983;73(1):133-136. doi:10.1111/j.1467-8306.1983.tb01400.x

36. Janpoor F, Torabian A, Khatibikamal V. Treatment of laundry waste-water by electrocoagulation. *J Chem Technol Biotechnol*. 2011;86:1113-1120. doi:10.1002/jctb.2625

37. Farhadi S, Aminzadeh B, Torabian A, Khatibikamal V, Alizadeh Fard M. Comparison of COD removal from pharmaceutical wastewater by electrocoagulation, photoelectrocoagulation, peroxi-electrocoagulation and peroxi-photoelectrocoagulation processes. *J Hazard Mater*. 2012;219-220:35-42. doi:10.1016/j.jhazmat.2012.03.013

38. Sander R. Compilation of Henry's law constants (version 4.0) for water as solvent. *Atmos Chem Phys*. 2015;15(8):4399-4981. doi:10.5194/acp-15-4399-2015

39. Moreno Casillas HA, Cocke DL, Gomes JA, et al. Electrochemistry Behind Electrocoagulation Using Iron Electrodes. 2007;6(9):1-15. doi:10.1149/1.2790397

40. Sasson M Ben, Calmano W, Adin A. Iron-oxidation processes in an electroflocculation (electrocoagulation) cell. *J Hazard Mater*. 2009;171(1-3):704-709. doi:10.1016/j.jhazmat.2009.06.057

41. Vernon L. Snoeyink DJ. Precipitation and Dissolution. In: *Water Chemistry*. 1st ed. Wiley; 1980:243-300.

Fig. 1. pH-pC diagrams showing the distribution of Fe(III) species in aqueous solution (left) and Fe(II) species in aqueous solution (right) for varying pH values.

159x111mm (96 x 96 DPI)

Fig. 2. Proposed mechanisms of ion exchange (A) Fe reaction with organic matter (OM, B) and carbonate stripping (C) leading to pH changes during EC.

259x122mm (150 x 150 DPI)

Fig. 3. Setup used for EC experiments. Dashed lines indicate electrical wiring.

213x114mm (95 x 95 DPI)

Fig. 4. Setup used for bubbling hydrogen. A is a syringe containing 0.1 M HCl, B is a flask containing magnesium turnings, C is the synthetic water, and D is a pH electrode.

80x64mm (143 x 143 DPI)

Fig. 5. pH related effects during EC plotted against the influent pH. (a) pH change during EC. Error bars represent standard deviations based on triplicate experiment. (b) Change in concentration of H^+ after EC treatment compensated for the buffer capacity encountered. The error bars represent standard deviations based on triplicate experiments. Note that the y-axis is logarithmic.

148x111mm (96 x 96 DPI)

Fig. 6. Change in H^+ concentration after EC treatment as a function of the charge loading applied to the sample. Note the multiplier at the top of the y axis.

99x80mm (96 x 96 DPI)

Fig. 7. Estimate of the potential impact of dissolved iron on the pH after EC, both in terms of (a) $\Delta[H^+]$ values and (b) ΔpH values with a buffer capacity of 450 µeq/L.

168x65mm (96 x 96 DPI)

Fig. 8. Change in pH over 72 hours of ion exchange in synthetic water solutions treated by EC. The error bars represent standard deviations based on triplicate experiments. The pH of the solutions was 6.00 prior to treatment.

218x138mm (96 x 96 DPI)

Fig. 9. Change in pH as a function of charge loading for three different concentrations of carbonate. The initial pH for this experiment was 6.00.

185x138mm (96 x 96 DPI)

Fig. 10. Change in pH as a function of time during bubbling with hydrogen gas for three different carbonate concentrations at three different initials pH values. The figure for pH 6 has been overlayed with the mean values of the results presented in Fig. 9 to show the similarities.

185x138mm (96 x 96 DPI)

Fig. 11. Change in buffer capacity as a function of time during the bubbling experiments. The initial pH for this experiment was 6.00.

115x92mm (96 x 96 DPI)

Fig. 12. Graph showing the development of equilibrium partial pressure of CO_2 as a function of pH at different total carbonate concentrations ranging from 225, 450, 675 and 900 µeq/L. Henrys constant is assumed to be 0.034 mol/(kgbar).

185x138mm (96 x 96 DPI)

Fig. 13. Change in pH after EC treatment. The title indicates the influent pH and EC configuration used for the experiment. Four different concentrations of humic acid (HA) were studied. The dotted lines represent the maximum theoretical pH change if all negative charges on HA were bound to Fe.

185x138mm (96 x 96 DPI)

Fig. A1. pH-pC diagrams for (a) Fe(III) species in aqueous solution and (b) Fe(II) species in aqueous solution. The corresponding OH^- release as a function of dissolved Fe is also shown.

159x111mm (96 x 96 DPI)

Fig. B1. EC cell dimensions and design

Fig. C1. Removal of carbonate during bubbling with H_2 gas as a function of time at different initial pH values. This assumes a hydrogen generation rate of 12 cm3/min as in the bubbling experiment, and corresponding to a dose of 105 C/L during a regular EC experiment. Note the multiplier at the top of the y axis.

185x138mm (96 x 96 DPI)

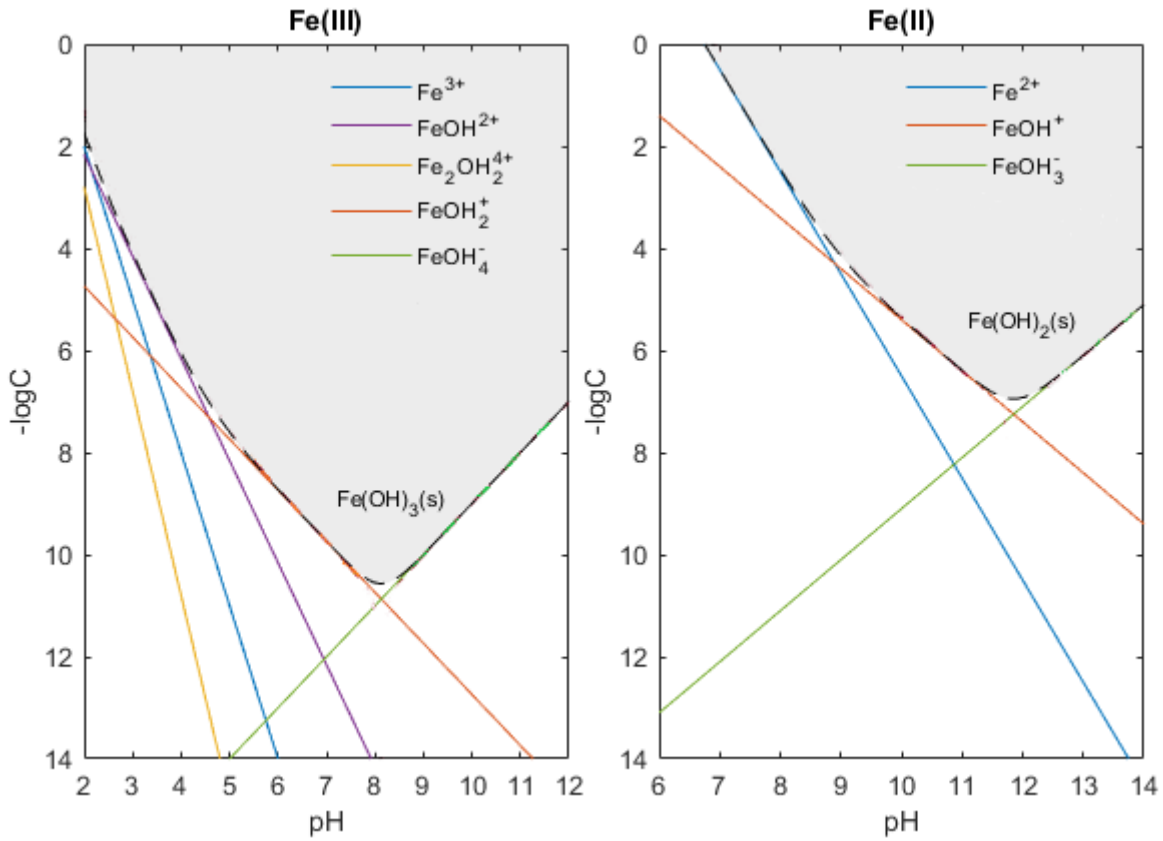

AIC_17384_Fig1.tif

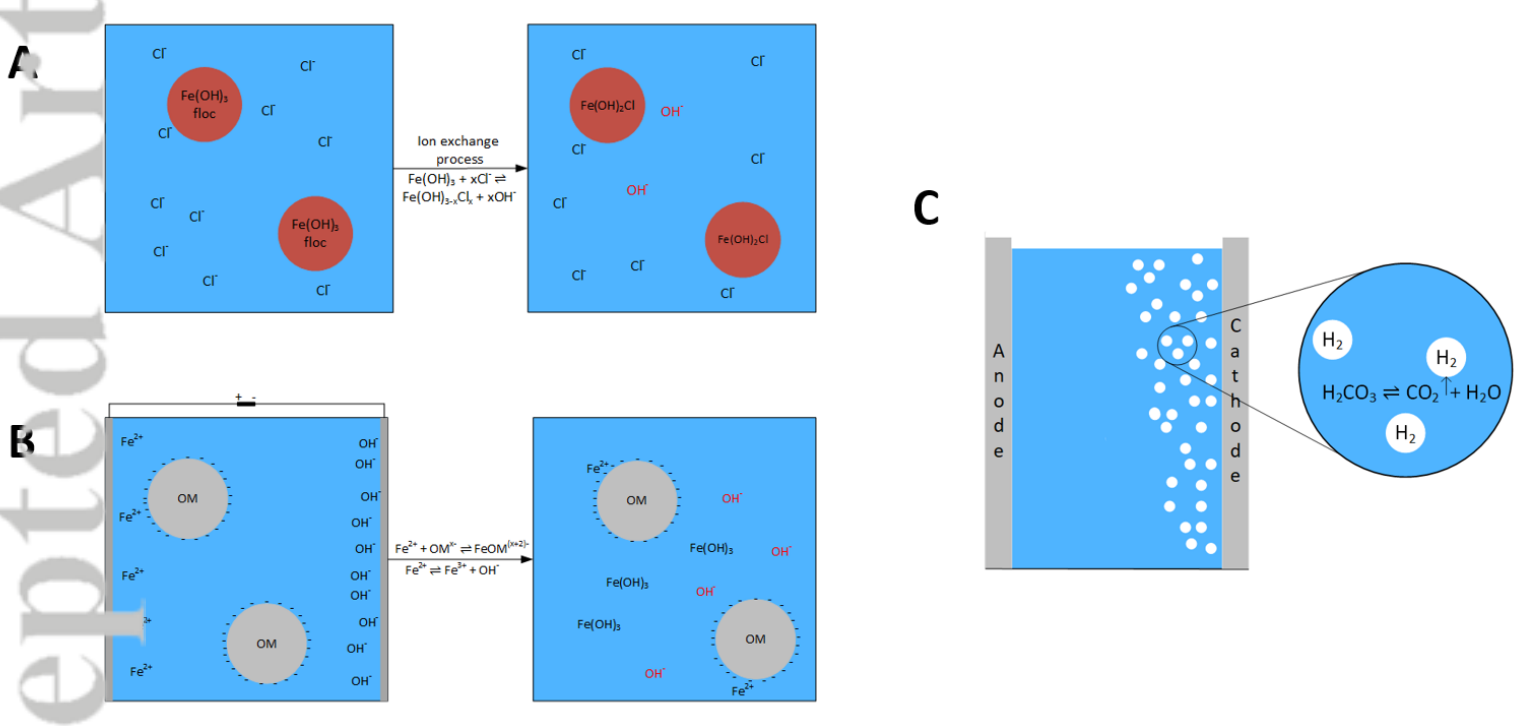

AIC_17384_Fig2.tif

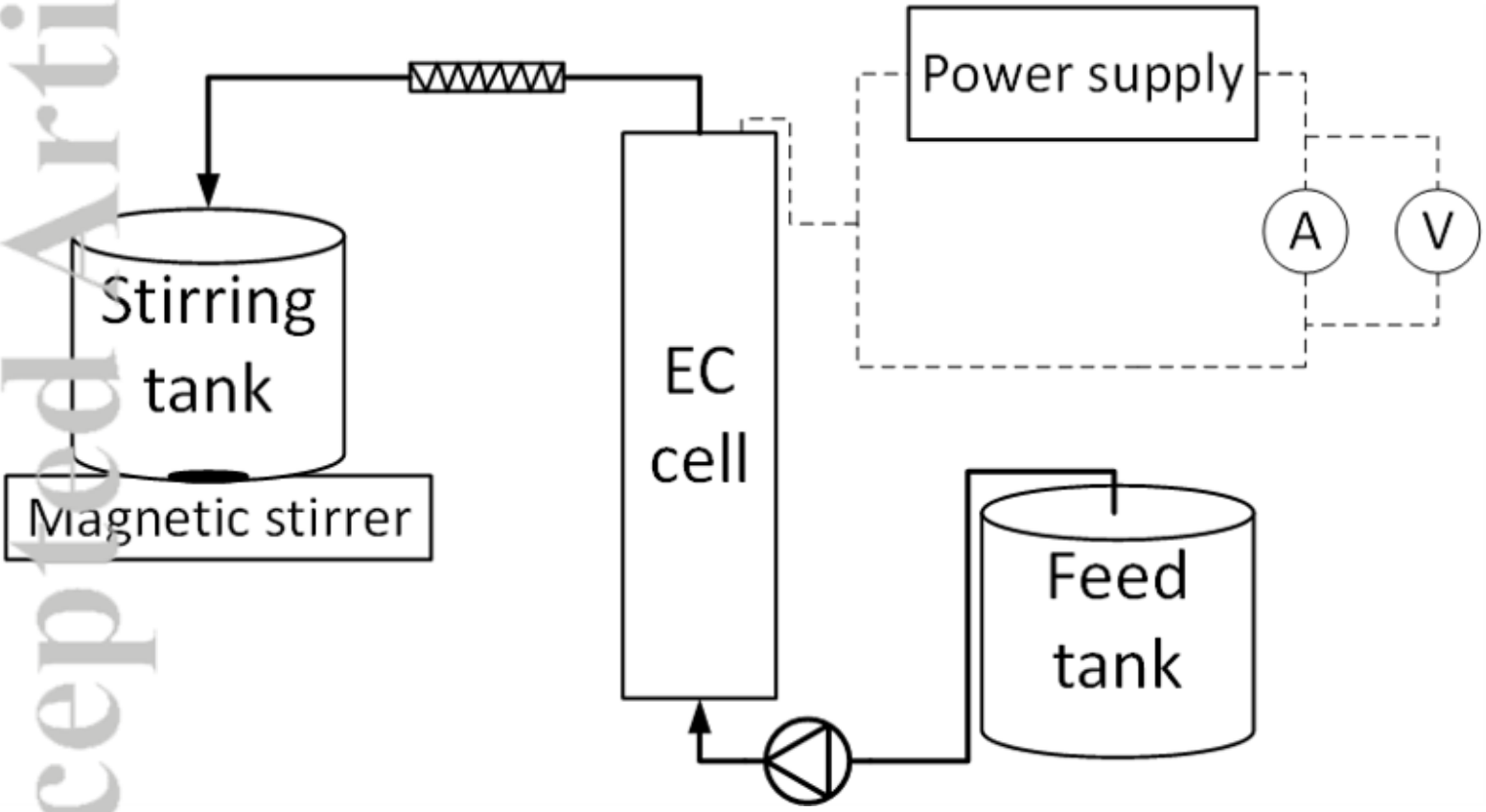

AIC_17384_Fig3.tif

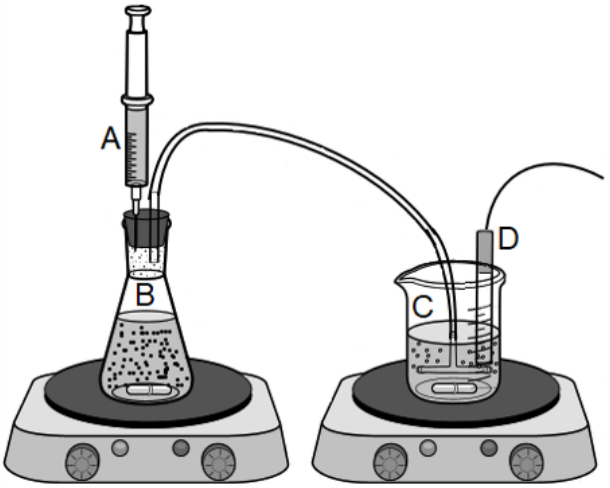

AIC_17384_Fig4.tif

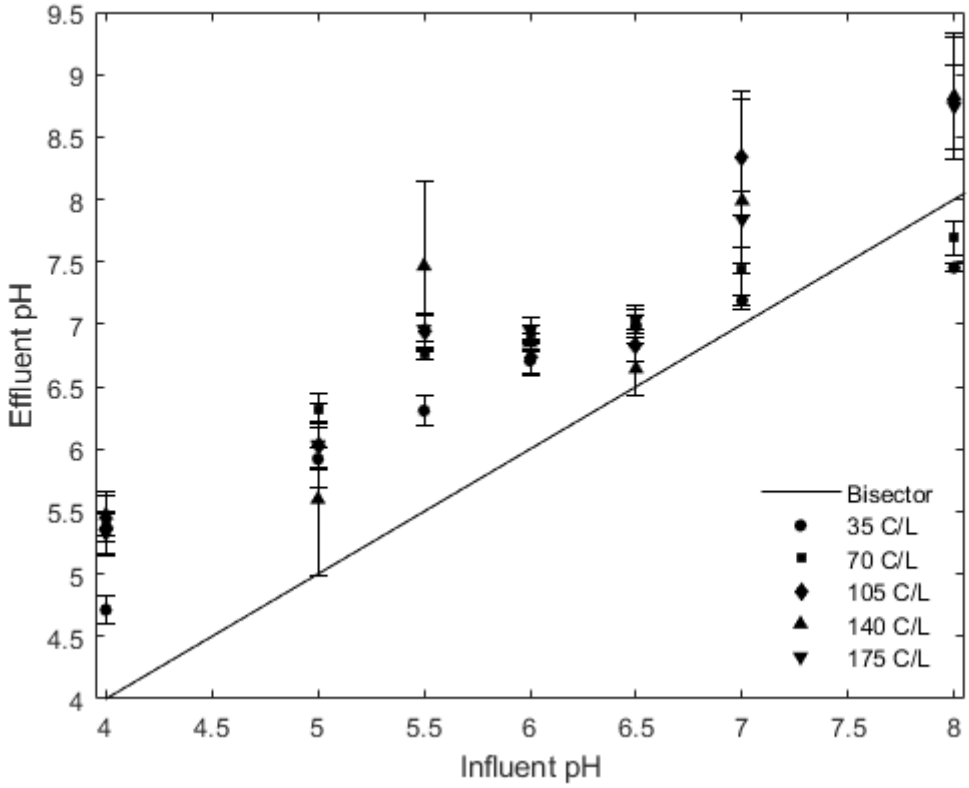

AIC_17384_Fig5a.tif

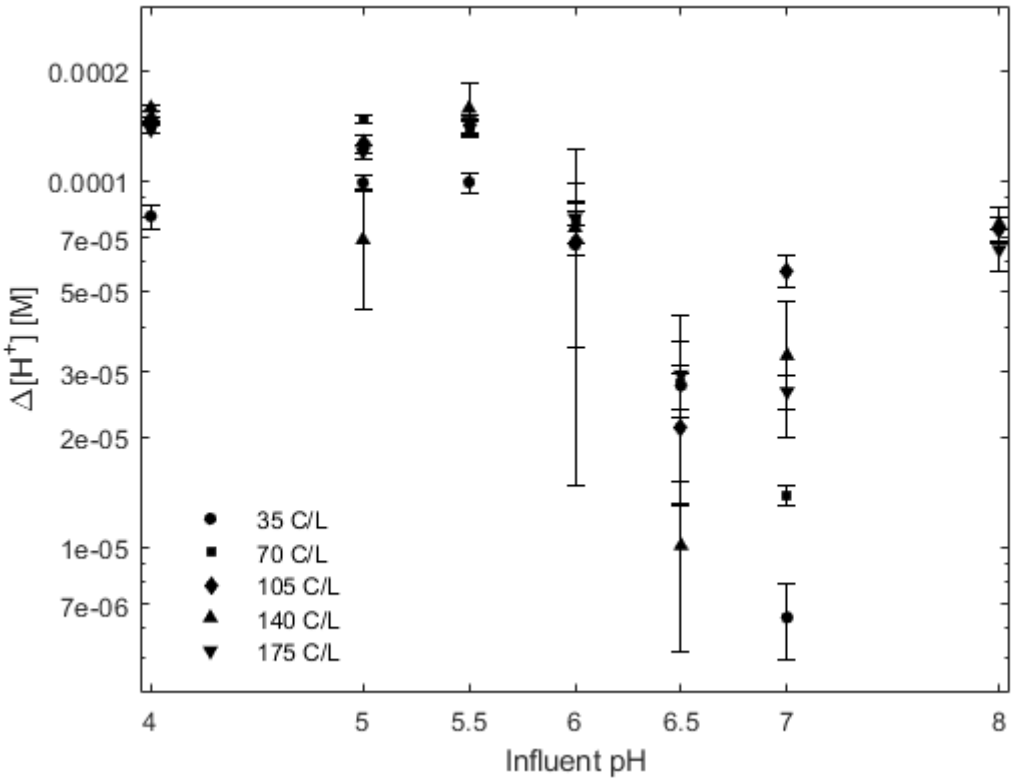

AIC_17384_Fig5b.tif

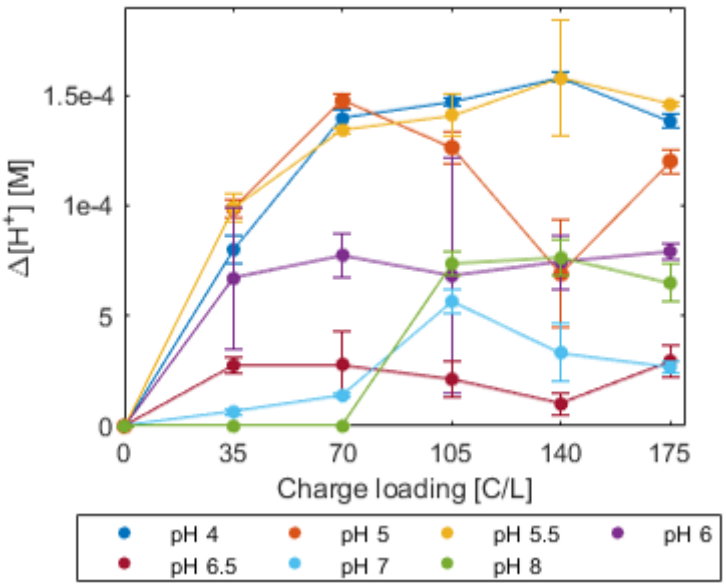

AIC_17384_Fig6.tif

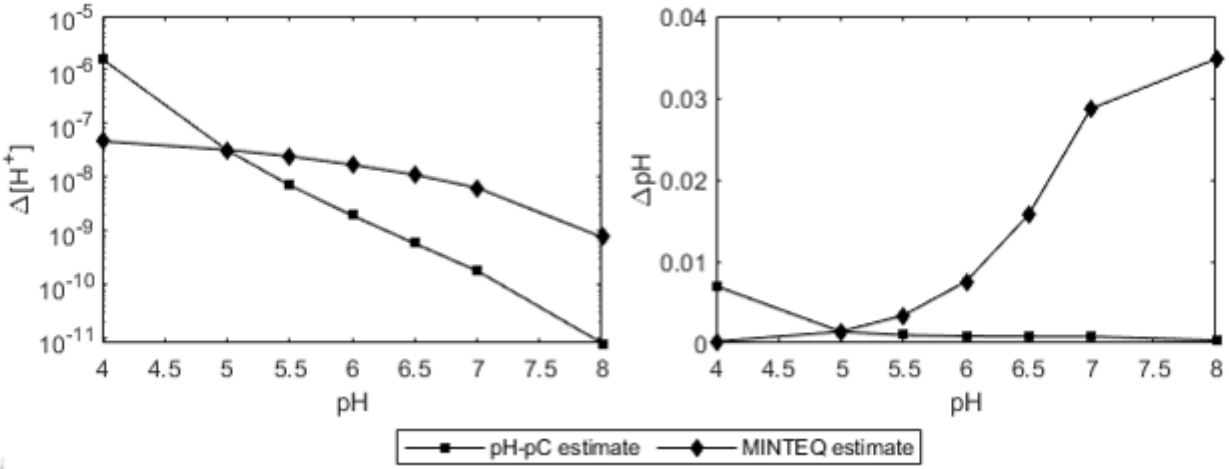

AIC_17384_Fig7.tif

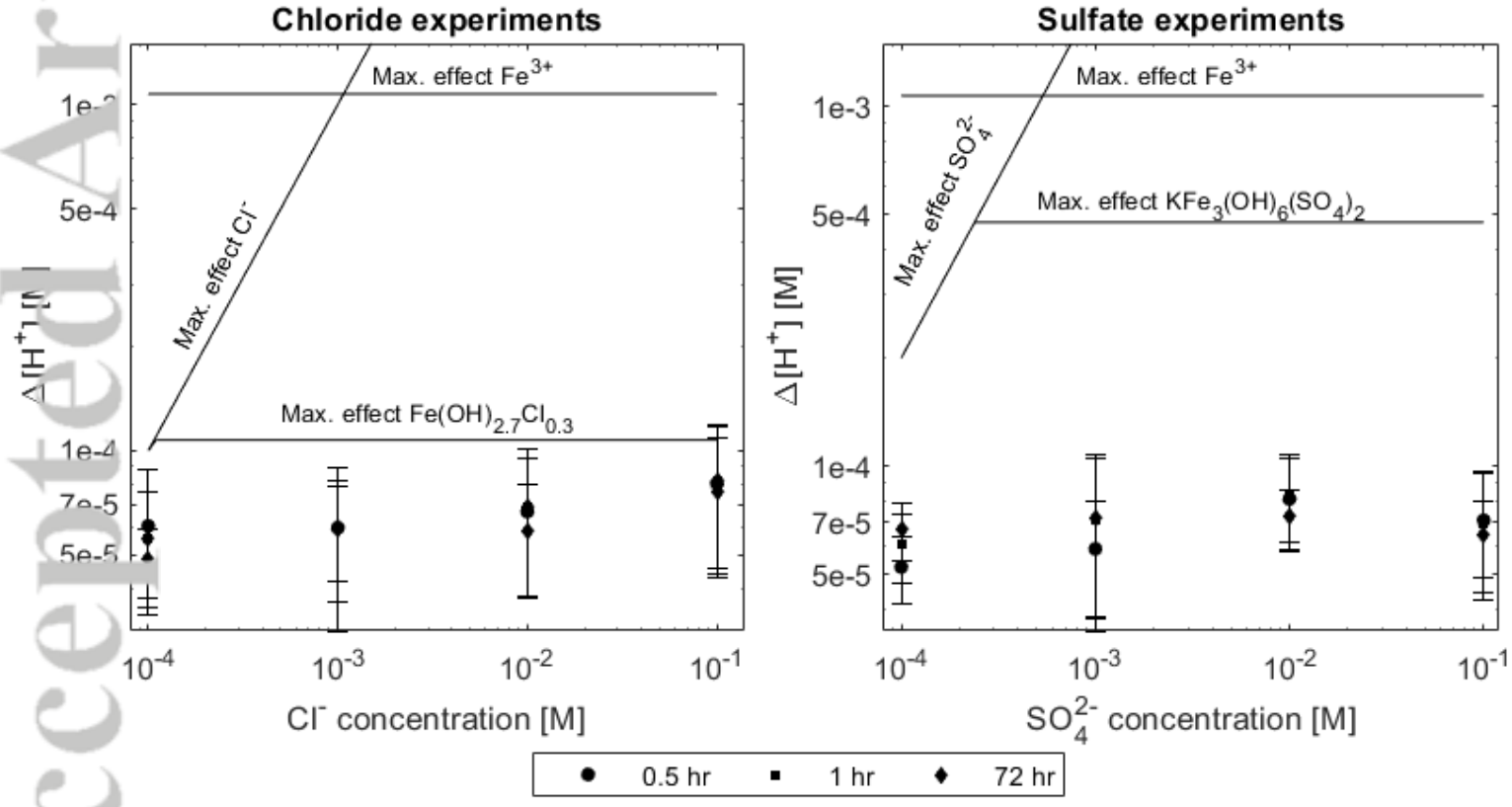

AIC_17384_Fig8.tif

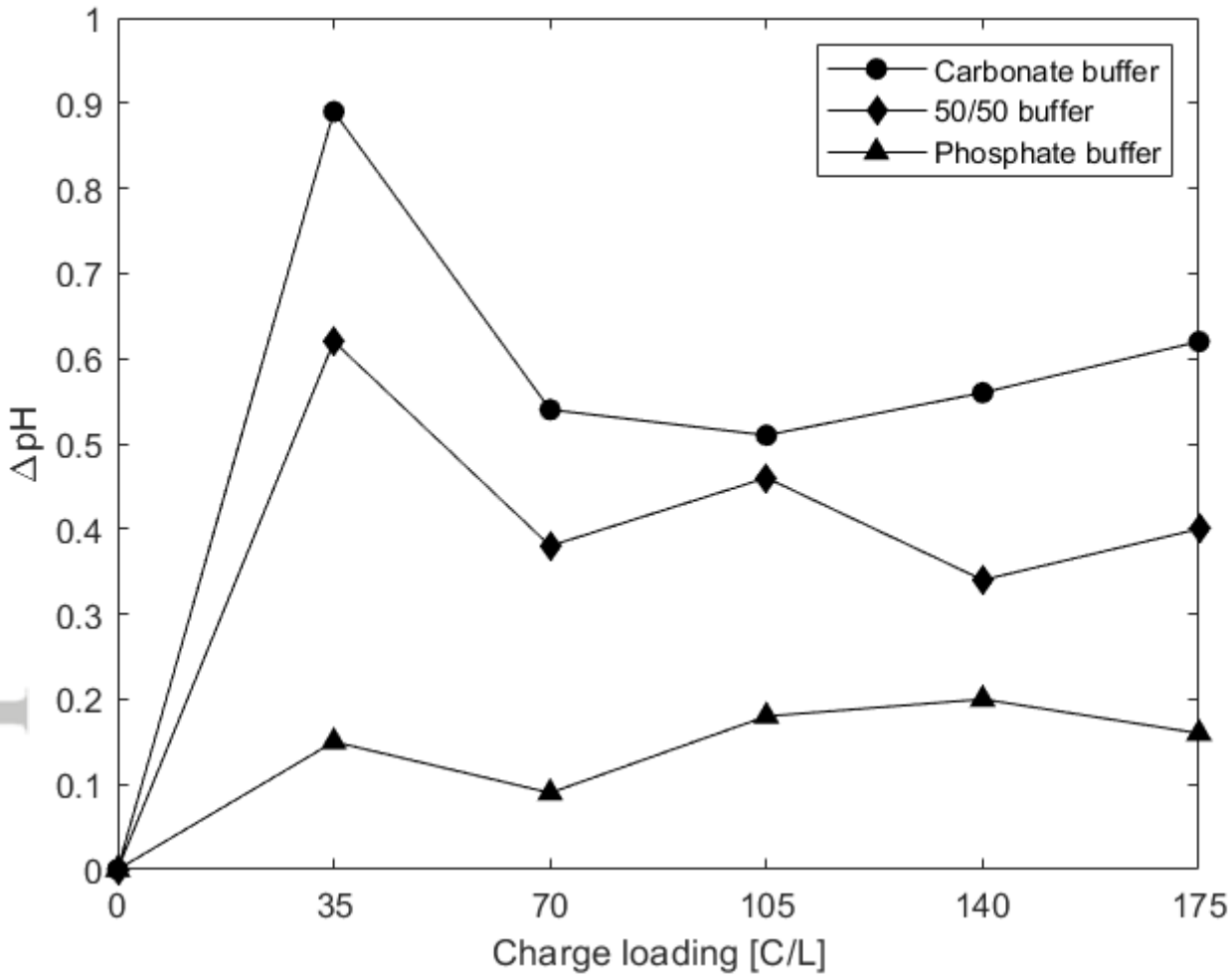

AIC_17384_Fig9.tif

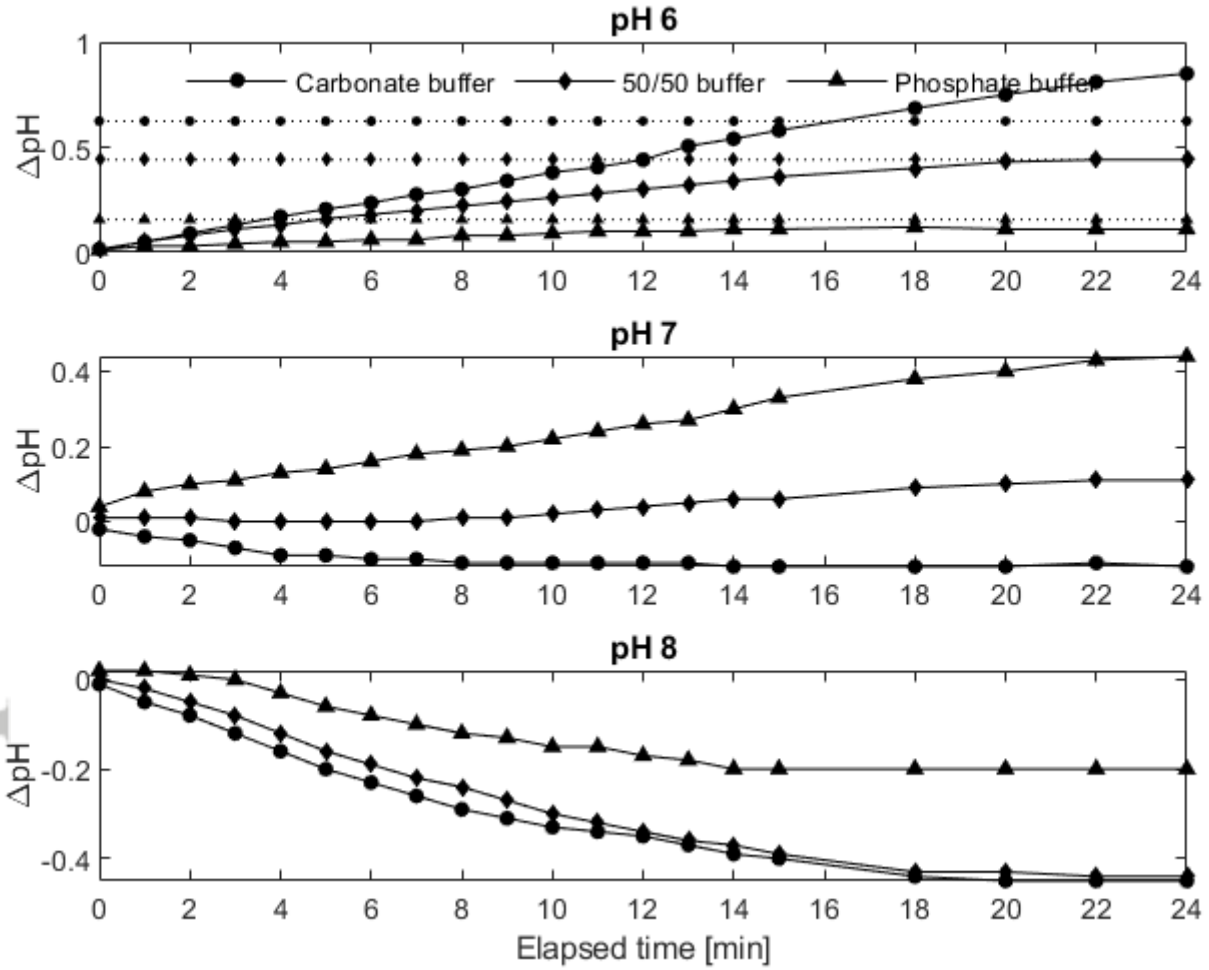

AIC_17384_Fig10.tif

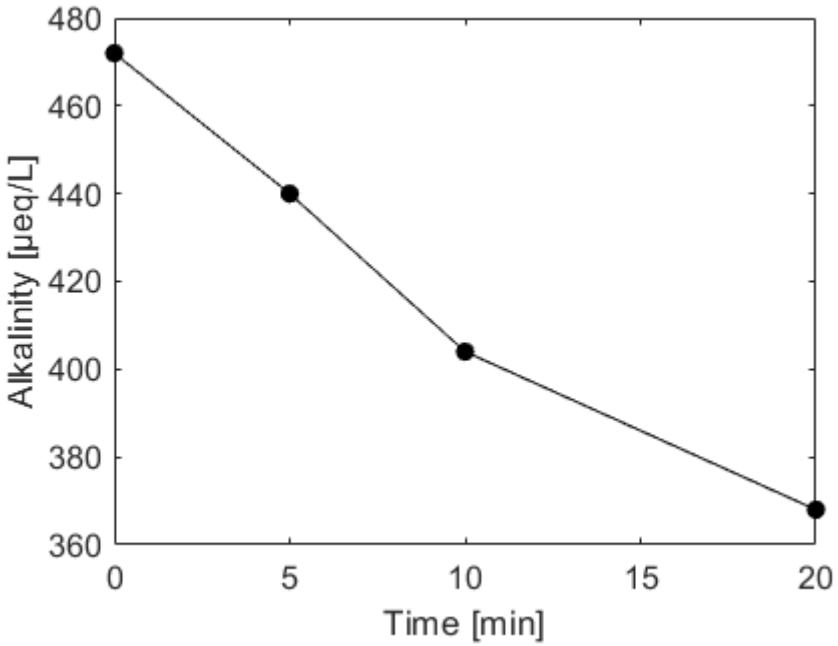

AIC_17384_Fig11.tif

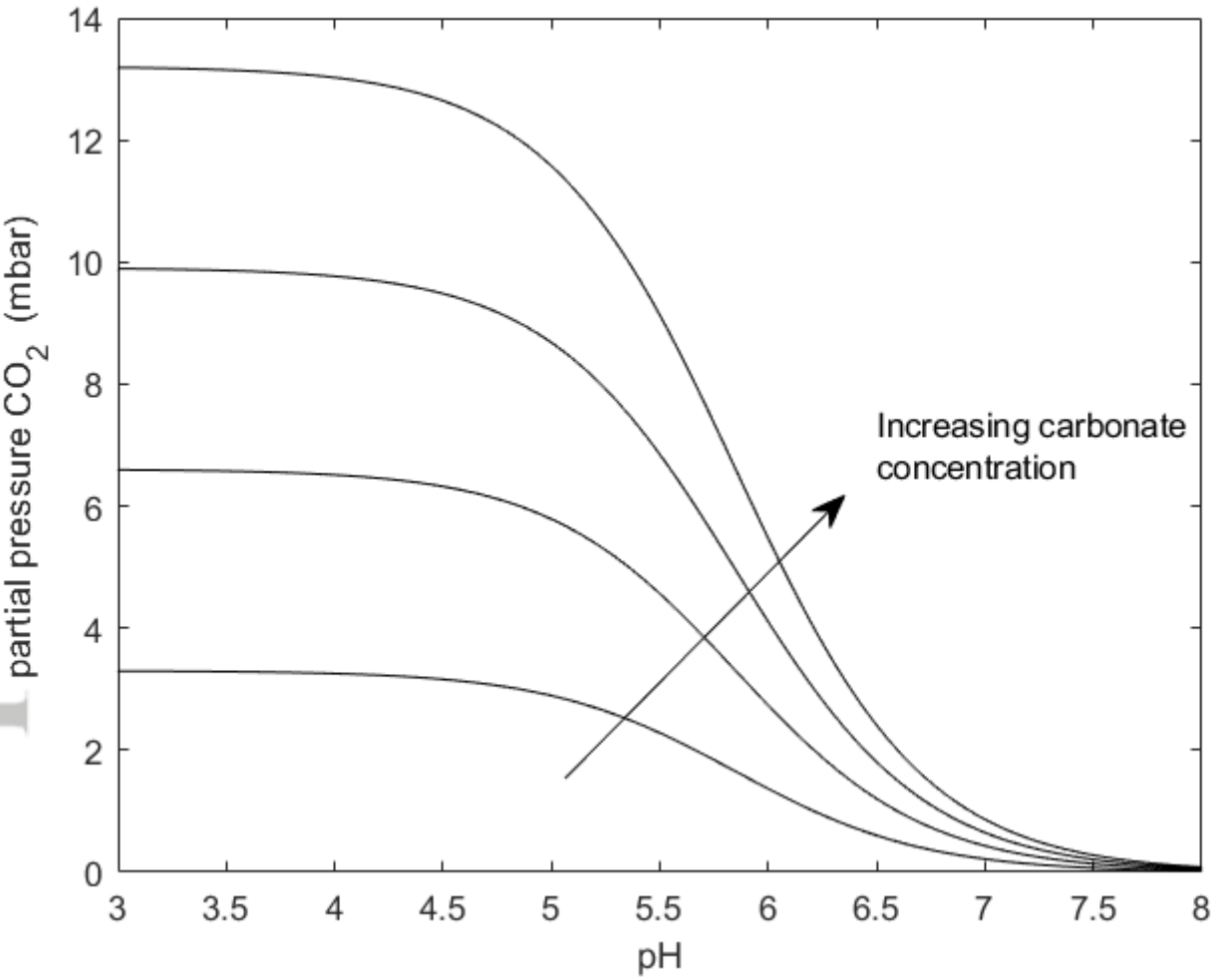

AIC_17384_Fig12.tif

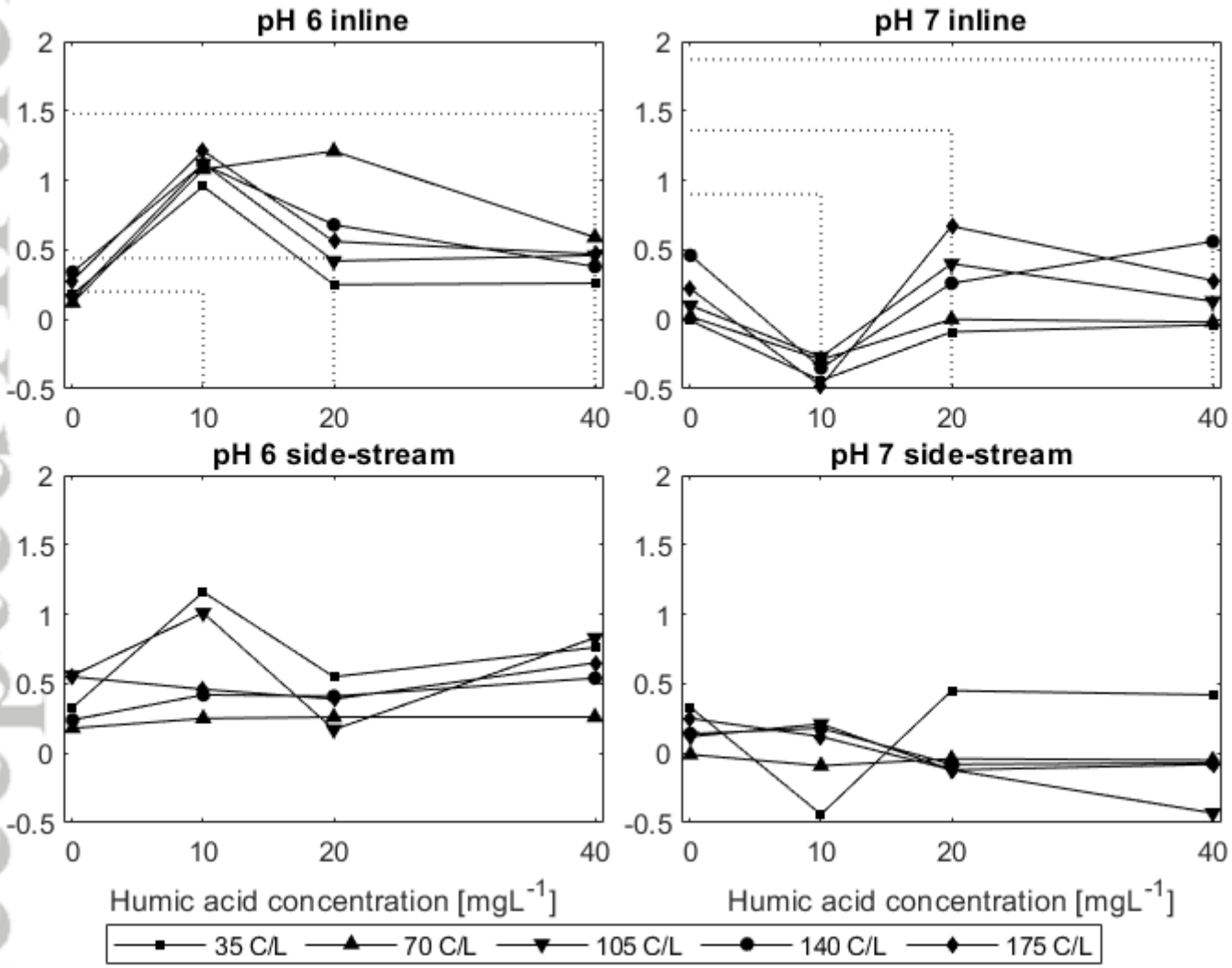

AIC_17384_Fig13.tif

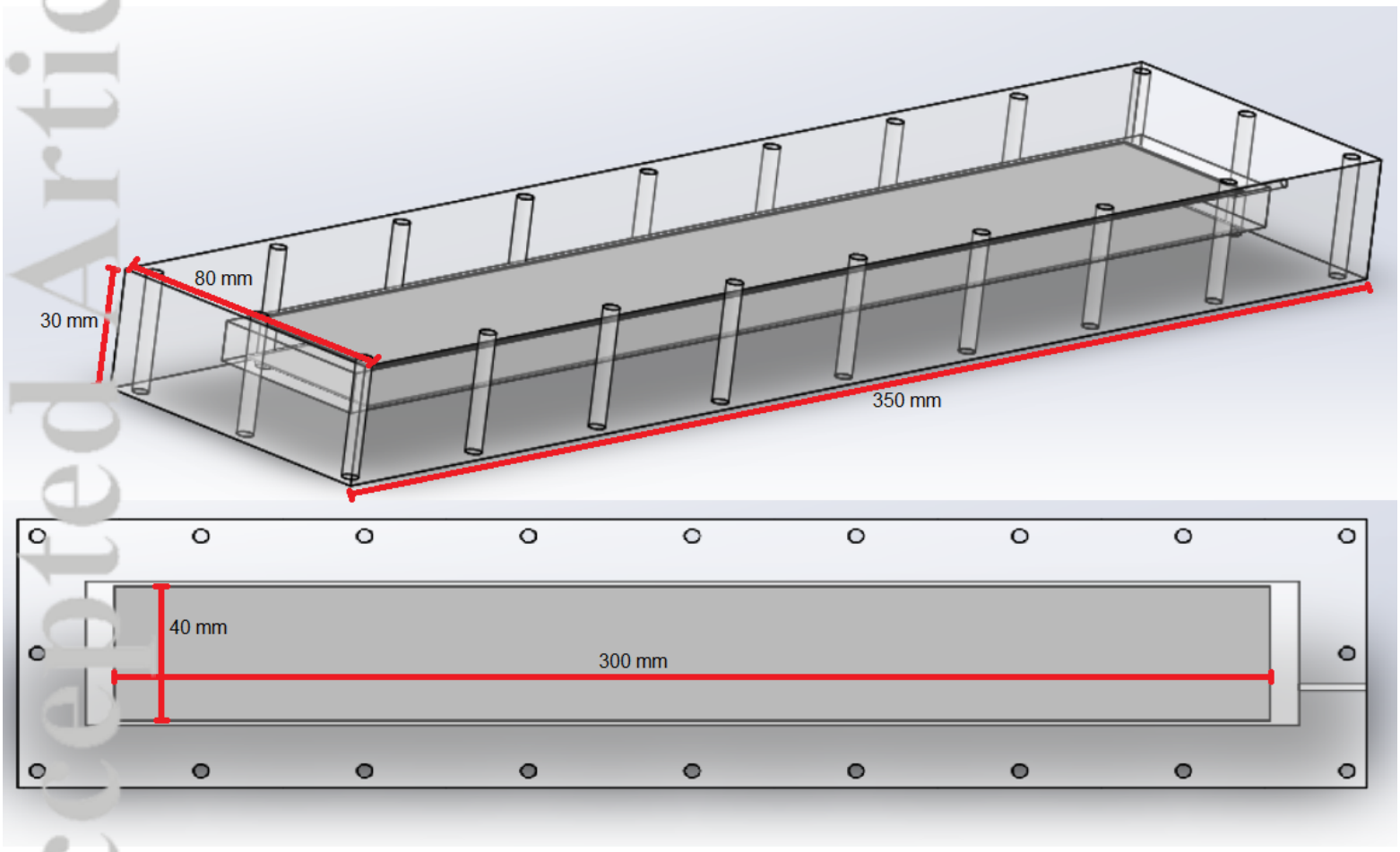

AIC_17384_Fig. B1.png

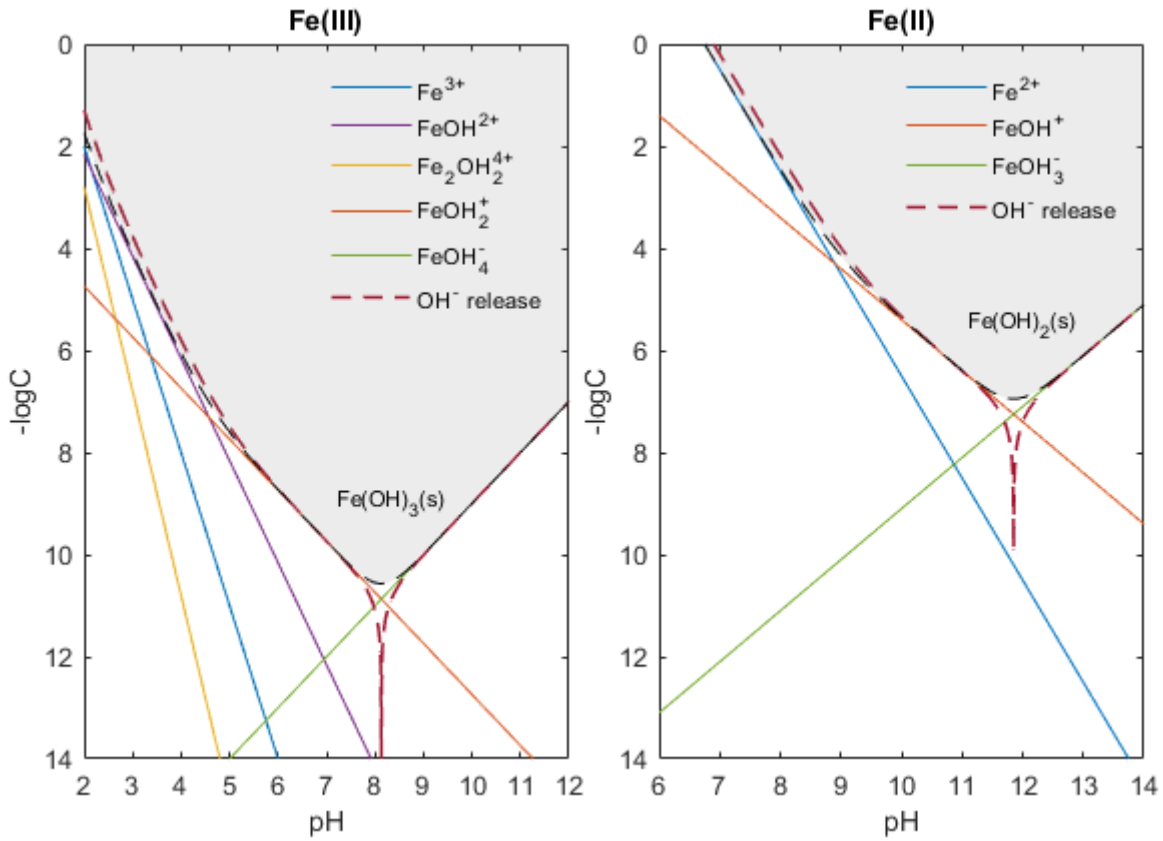

AIC_17384_FigA1.tif

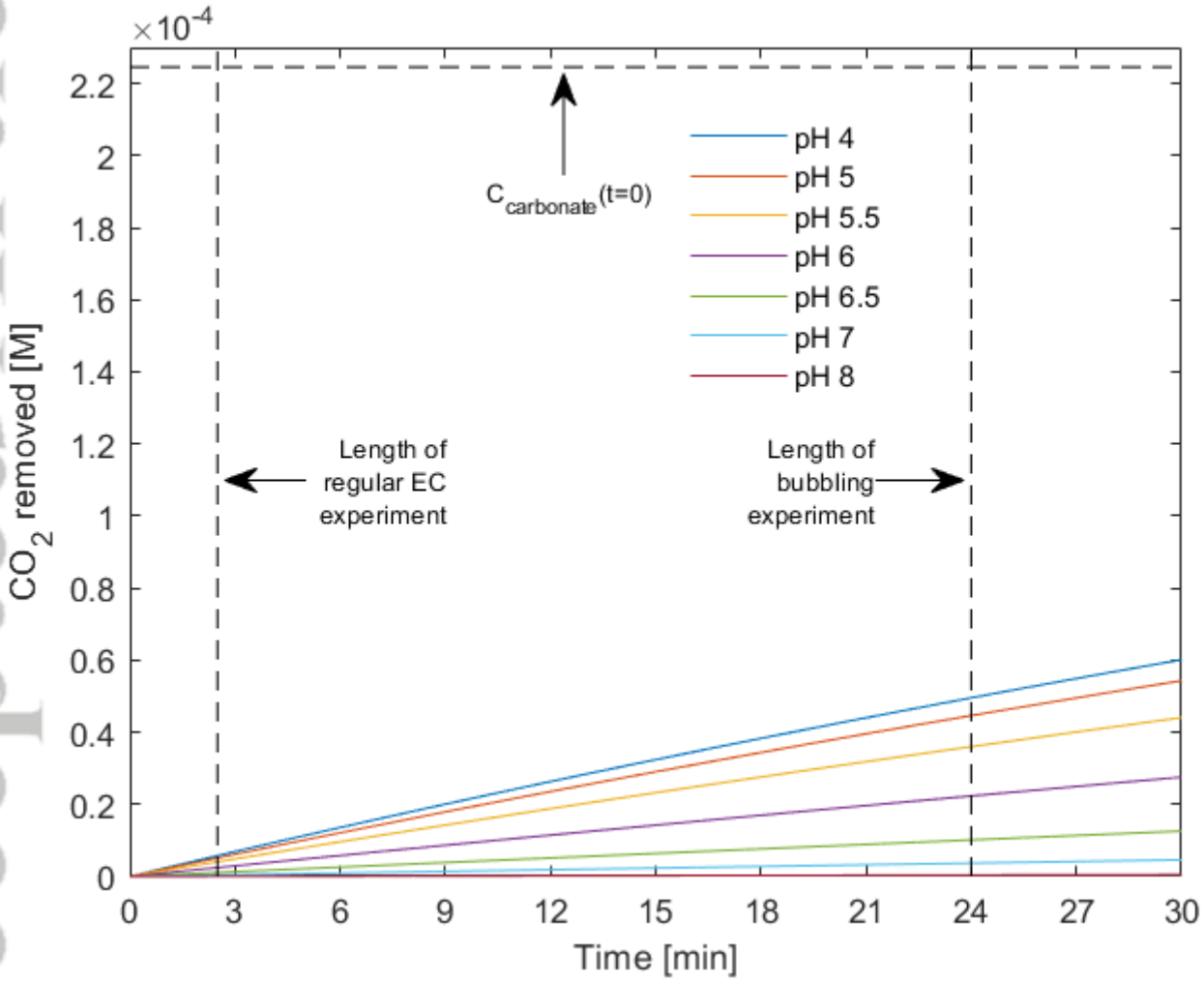

AIC_17384_FigC1.tif

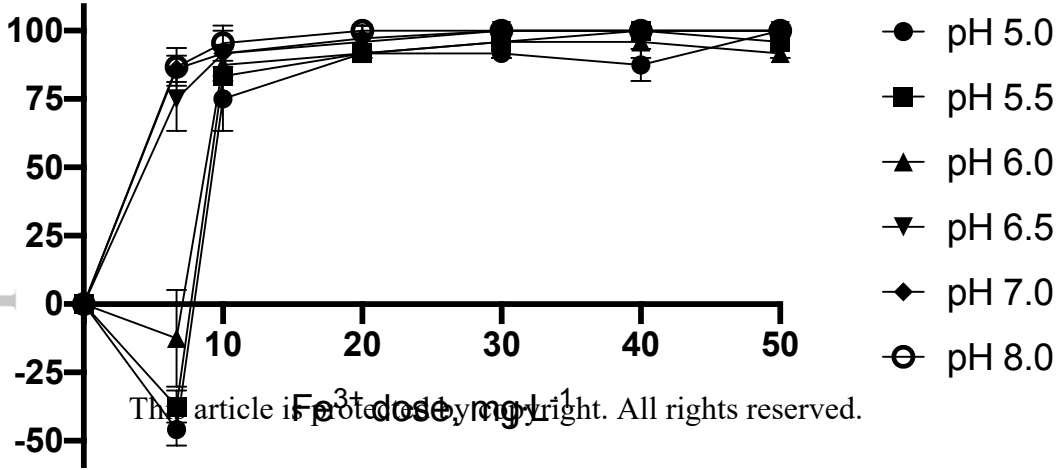

Table 1. Advantages and disadvantages of EC compared to CC.

Advantages	**Disadvantages**
Gas bubbles formed during EC promote flotation of pollutants [10,12].	Energy requirements for EC are dependent on the electrical conductivity of treated water [12].
No pollution with SO_4^{2-} or Cl^-, since no chemicals are added [10].	Electrode passivation can lead to low efficiency of the EC process [10,13].
Some studies have shown that EC is cheaper to operate than CC [14–16].	Operating costs fluctuate with daily electricity prices.
Efficient in a broader range of pH values [17,18].	Toxic chlorinated organic compounds can be formed during EC [12].

Table 2. Constituents of the synthetic surface water used for this study.

Constituent	Concentration
Na^+	5.31 mg/L
Mg^{2+}	2.81 mg/L
K^+	0.94 mg/L
Ca^{2+}	11.22 mg/L
SO_4^{2-}	11.01 mg/L
NO_3^-	2.51 mg/L
Cl^-	20.7 mg/L
Humic acid	10.0 mg/L
Carbonate	0-450 µeq/L
Phosphate	0-450 µeq/L

Table 3. Overview of experiments to investigate mechanism behind pH change during EC.

	Ion exchange mechanism	Hydrogen gas stripping mechanism 1	Hydrogen gas stripping mechanism 2	Reactions between Fe^{2+} and Organic Matter
Charge loading	70 C/L	0 – 175 C/L		70 C/L
Sampling	Measure pH before and 30 min, 60 min and 72h after EC dosage	Measure pH before and during EC	Measure pH before and during H_2 sparging	Measure pH before and 25 min after EC
Initial pH	6.00	6.00, 7.00 and 8.00	6.00, 7.00 and 8.00	6.00 and 7.00
Buffer capacity		450 µeq/L with different contributions from carbonate and phosphate	450 µeq/L with different contributions from carbonate and phosphate	
Specific settings	Sulfate and chloride ion concentrations: 10^{-4} M, 10^{-3} M, 10^{-2} M, and 10^{-1} M		H_2 sparged in amount corresponding to EC charge loading of 105 C/L.	HA of 0, 10, 20, and 40 mg/L

Table 4. Composition of the different buffering systems employed in this study.

Buffer system	**Carbonate concentration**	**Phosphate concentration**
Carbonate	450 µeq/L	0 µeq/L
50/50 buffer	225 µeq/L	225 µeq/L
Phosphate	0 µeq/L	450 µeq/L